Vol 16 No 12, December 2007
1009-1963/2007/16(12)/3868-05
Chinese Physics
© 2007 Chin. Phys. Soc.
and IOP Publishing Ltd

Growth parameter dependence of magnetic property of CrAs thin film*

Bi Jing-Feng(毕京锋)[a], Zhao Jian-Hua(赵建华)[a]†, Deng Jia-Jun(邓加军)[b,a], Zheng Yu-Hong(郑玉宏)[a], Wang Wei-Zhu(王玮竹)[a], Lu Jun(鲁 军)[a], Ji Yang(姬 扬)[a], and Li Shu-Shen(李树深)[a]

[a] *State Key Laboratory for Superlattices and Microstructures, Institute of Semiconductors, Chinese Academy of Sciences, Beijing* 100083, *China*

[b] *Department of Physics, University of Science and Technology of China, Hefei* 230026 *China*

(Received 11 January 2007; revised manuscript received 26 February 2007)

This paper has systematically investigated the substrate temperature and thickness dependence of surface morphology and magnetic property of CrAs compound films grown on GaAs by molecular-beam epitaxy. It finds that the substrate temperature affects the surface morphology and magnetic property of CrAs thin film more potently than the thickness.

Keywords: magnetic films, zinc-blende CrAs, room-temperature ferromagnetism, molecular-beam epitaxy

PACC: 7570, 6000, 7550P, 8115

1. Introduction

Since the first discovery by de Groot and his collaborators in the early 1980s, several kinds of half-metallic ferromagnets (HMFs), such as Heusler alloys NiMnSb,[1] magnetite Fe_3O_4,[2] rutile-type CrO_2,[3] perovskite manganite $La_{1-x}Sr_xMnO_3$[4] and diluted magnetic semiconductors (Ga,Mn)As[5−8] have been reported. In these materials, one spin channel is metallic while the other is insulating, and they may provide 100% spin-polarization. Therefore, HMFs have been expected to play a key role in the next-generation spintronic devices. However, these potential candidates show some vital disadvantages, for examples, lower Curie temperature (T_c), conductivity mismatch with semiconductors, difficulties in controlling the stoichiometry, and non-half-metallic surface, all these vital disadvantages restrict their practical applications.

A new class of prospective half metal is zinc-blende transition-metal pinctide, like zinc-blende CrAs (zb-CrAs), zb-MnAs and zb-CrSb, which are room-temperature ferromagnetic and compatible with ordinary III-V semiconductors. Among them, zb-CrAs is the most favoured candidate for spin injection into GaAs-based semiconductors since its lattice constant is close to that of GaAs and the degree of spin polarization is not reduced significantly by atomic disorder or the atomic diffusion at the interface.[9−14] Akinaga *et al* firstly grew CrAs thin films on GaAs (001) substrates and found CrAs to be a ferromagnet having T_c higher than 400 K.[15] This discovery aroused the interest of researchers to grow this novel kind of compound.[15−18]

Zb-CrAs is a metastable phase, and its structure and magnetic properties strongly depend on growth conditions. However, only few works have dealt with the relationship between growth parameters and structural and magnetic properties of zb-CrAs so far.[19,20] To realize its practical application in spintronic devices, comprehensive understanding on growth parameter dependence of structural and magnetic characterization of zb-CrAs is a prerequisite. Using the low-temperature molecular-beam epitaxy (MBE) technique, we obtained zb-CrAs thin films with high quality and observed room-temperature ferromagnetism existing in them. This result clarified the controversy about the origin of the room-temperature ferromagnetism in CrAs compounds.[15,21,22] Based on the previous work, we have systematically studied the influence of growth parameter on structural and magnetic property of zb-CrAs. In this paper, we report

*Project supported by the National Natural Science Foundation of China (Grant Nos 10334030, 10425419 and 60521001).
†E-mail: jhzhao@red.semi.ac.cn

growth temperature and film-thickness dependence of surface morphology, structural and magnetic properties of CrAs compounds.

2. Experiments

The CrAs thin films were grown on the semi-insulating GaAs (001) substrates employing a V80MARKI MBE system. The GaAs wafers were set on molybdenum holders with indium solder. Surface reconstruction was monitored by reflection high-energy electron diffraction (RHEED) at 11 keV during all the growth processes and the substrate temperature T_S was measured by a W-Re thermal couple.

After the surface oxide layer was removed at substrate temperature $T_S = 580\,^\circ$C, a GaAs buffer layer with the thickness of 300 nm was grown at 560 °C, and the typical streaky (2×4) RHEED pattern was observed. The As shutter was closed when the T_S decreased to 400 °C to avoid the buildup of the As. Then the CrAs films were grown by opening the shutters of the As and Cr effusion cells simultaneously with the intended growth parameters such as different growth rate, growth time, and T_S. Here, we grew two sets of CrAs thin films by using the growth rate of 1.74 nm/min and the As/Cr beam ratio of 400. The first set of samples are those with different nominal thickness of 1 nm (sample A), 3 nm (sample B) and 5.6 nm (sample C), were grown at 250 °C. And the second set of samples are those with the same thickness of 3 nm but different T_S of 150 °C (sample D), 250 °C (sample E), and 350 °C (sample F), respectively. The initial bright RHEED pattern became gradually weak and only the shadow can be seen during the growth of samples A, B and C. If the thickness was larger than 5.6 nm, some non-zincblende spots would appear. RHEED patterns during the growth of samples D and E evolved with the similar trend as that of the first set of samples. As to sample F, the evolution of RHEED pattern was different from those of samples D and E, and the quite complicated spotty pattern appeared when the thickness was near 3 nm. For all the CrAs films, when the low-temperature GaAs cap layers were grown on them, a RHEED pattern of amorphous or poly-crystalline characterization would appear.

The surface morphologies were analysed by *ex situ* atomic force microscopy (AFM). The magnetic properties were measured by superconducting quantum interference device (SQUID). The cross-sectional high-resolution transmission electron microscopy (HRTEM) images were taken by the system of JEM-2010F.

3. Results and discussion

3.1. Surface morphology

To ascertain the thickness and substrate temperature dependence of structural characteristics of CrAs thin films, surface morphologies of the six samples were investigated by AFM. The surface morphologies of samples A, B and C are similar. With the increase of the thickness, the surface keeps relatively smooth and no obvious change appears. The root mean square (RMS) of surface roughness for samples A, B and C is 0.265 nm, 0.249 nm and 0.212 nm, respectively, as shown in Figs.1(a), 1(b) and 1(c). However, the situation becomes different as to samples D, E and F, which were grown at different T_S. Figures 2(a), 2(b) and 2(c) show the surface morphologies of the CrAs grown at 150 °C, 250 °C and 350 °C, respectively. We know that the atomic surface diffusion length l_S is given by $l_S = \sqrt{2D_S\tau_S}$, where $D_S = D_0\exp(-E/kT)$ is the thermally activated surface diffusion coefficient and τ_S is the mean residence time of adatoms. A reduction of the effective surface diffusion length l_S is generally obtained by reducing the substrate temperature, but this may have a deleterious effect on material quality.[21] A rough surface is observed in sample D (see Fig.2(a)), with the CrAs film grown at T_S =150 °C. We assume this condition to be attributed to the strained situation, that is, the source atoms have low D_S and there is not enough energy for diffusion at low T_S. So the surface morphology changes because of the nucleation of islands in the growing layers relieving the strain by dislocations. Here, the RMS roughness is about 0.343 nm. When the T_S has a raise to 250 °C (sample E), higher kinetic energy induces higherD_S and longer l_S as shown in Fig.2(b). The strain originated by the slight lattice mismatch between CaAs and CrAs has been relaxed to some extent. The RMS roughness of sample E is 0.236 nm, which is a little smaller than that of sample D. A relatively flat surface is observed in sample F grown at $T_S = 350\,^\circ$C. The RMS roughness is 0.215 nm, which is the smallest of three samples. In this condition, the relaxation occurs and the strain has been relieved totally. Only tiny islands disperse in the whole surface as shown in Fig.2(c). A thermodynamic balance exists

for the corresponding strain relaxation conditions in every situation. So the substrate temperature affects the surface morphology most directly, and the surface keeps the trend of being flat with the increase of substrate temperature. At higher substrate temperature, the thermal stable phase can be built easier but the zinc-blende structure can also be easier to be relaxed into non-zinc-blende structure. Considering all these conditions, we take 250 °C to be the optimal substrate temperature to grow zb-CrAs films.

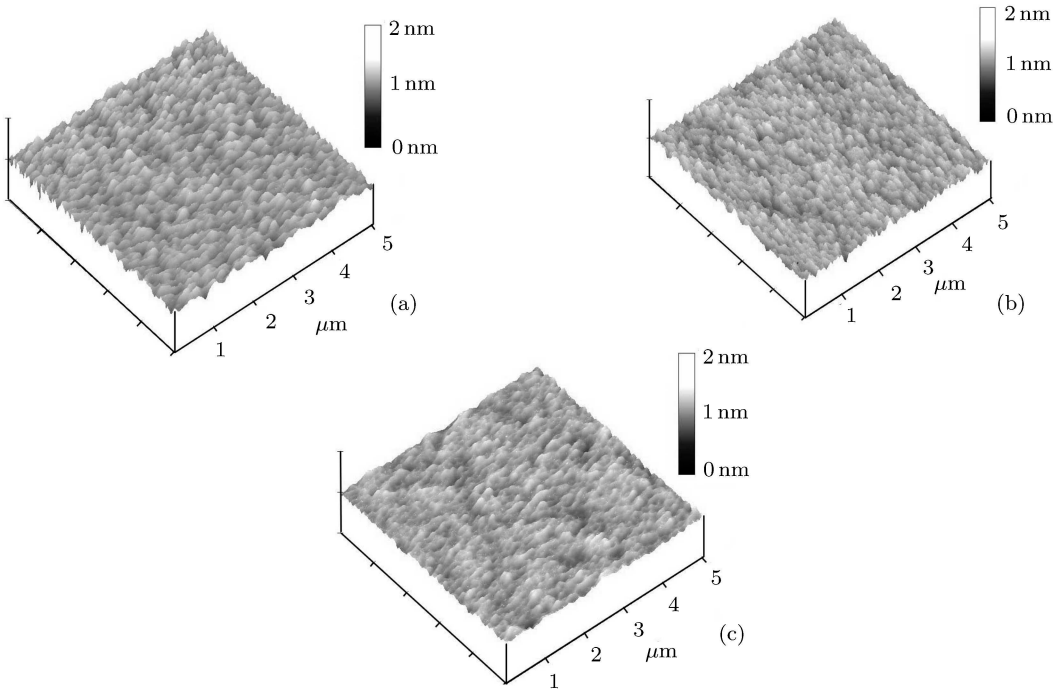


Fig.1. Surface morphologies of CrAs thin films of sample A (a), sample B (b) and sample C (c).

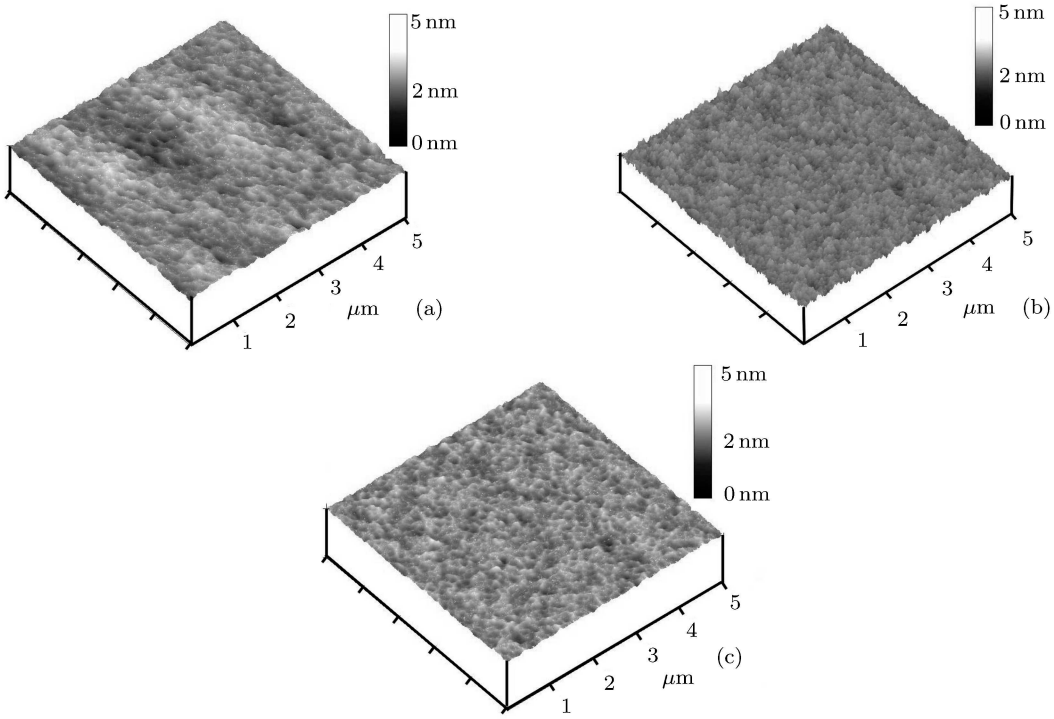


Fig.2. Surface morphologies of CrAs thins films grown at 150 °C ((a), sample D), 250 °C ((b), sample E) and 350 °C ((c), sample F).

3.2. Magnetic property

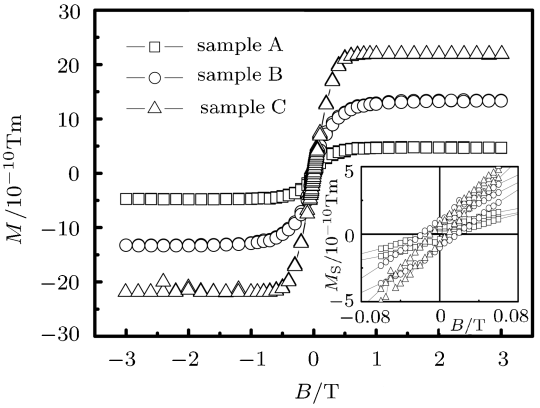


Fig.3. Magnetic field dependence of magnetization of samples A (square), B (circles) and C (triangles) at 300 K under magnetic field parallel to the sample surface. The right inset is an enlargement of the hysteresis around zero magnetic field at 300 K.

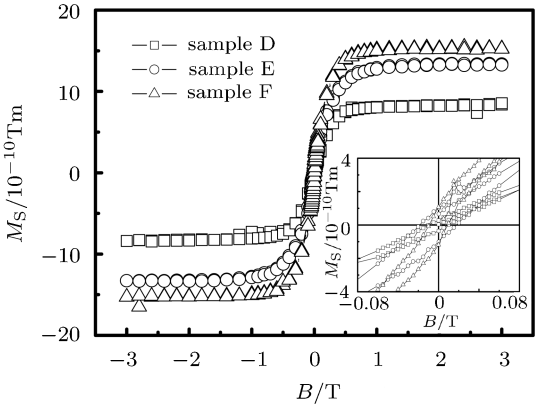


Fig.4. Magnetic field dependence of magnetization of samples D (square), E (circles) and F (triangles) at 300 K under magnetic field parallel to the sample surface. The left inset is an enlargement of the hysteresis around zero magnetic field at 300 K.

The magnetic properties are characterized by SQUID magnetometer. Figures 3 and 4 show the magnetic field dependence of magnetization per unit area M of all the samples measured at 300 K under magnetic field B parallel to the surface of the sample. The applied magnetic field is 3 T and strong enough to saturate magnetization. The soft but clear hysteresis at 300 K reveals that room-temperature ferromagnetism exists in all the samples. The antimagnetic contribution of the GaAs substrates and buffer layers has been subtracted from all the data. The curves of remanent magnetization per unit area M_r versus temperature T from 5 to 400 K of all the samples shown in the Fig.5 indicate that the T_c of these samples exceeds 400 K. Actually, the Curie temperature has not yet been determined because of the operating-temperature limit of the SQUID magnetometer.

The right inset of Fig.3 is the enlargement of the hysteresis loops at 300 K around zero magnetic field. We can see that the coercive force of three samples are very small (16 kA/m). If we assume the effective magnetization per Cr atom in zb-CrAs to be 3 μ_B (μ_B: Bohr magneton) and $g = 2$ of Landé g-factor of Cr, the magnetization of each monolayer of zb-CrAs should be 2.2×10^{-10} Tm. Based on this assumption and the saturation magnetization M_s at 5 K, 4.89×10^{-10} Tm (sample A), 18.67×10^{-10} Tm (sample B), 29.65×10^{-10} Tm (Sample C), the thickness of zb-CrAs in sample A, B and C is calculated to be ∼1, 3 and 5.6 nm respectively. The inset of Fig.4 is the enlargement of the hysteresis loops at 300 K around zero magnetic field. Also the coercive force is no more than 16 kA/m. Using the same method mentioned above, we have calculated the thickness of zb-CrAs in sample D, E and F to be ∼1.5, 3 and 3.5 nm respectively. The thickness deduced from the saturation magnetization at 5 K is much less than the nominal thickness determined by the growth parameter in sample D, which might result from the formation of a nonferromagnetic phase during the growth at the low T_S.

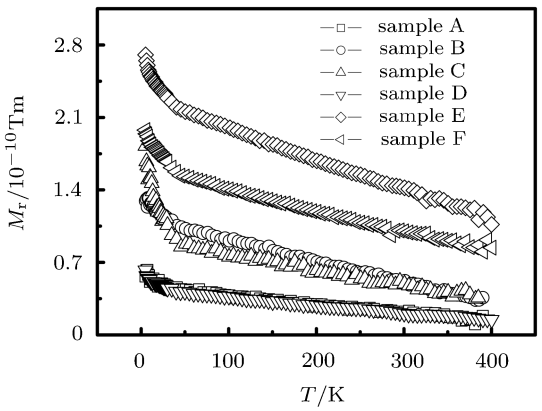


Fig.5. The temperature dependence of remanent magnetization of sample A, B, C, D, E and F under zero magnetic field.

Remanent magnetization versus temperature curves decrease smoothly for other samples. However there is a turning point at about 50 K in the curve of sample C in Fig.5. The thickness deduced from the magnetic properties of sample C is larger than the thickness of zb-CrAs determined from HRTEM images (see Fig.6). We can see that two parts marked I and II represent CrAs compounds with two different structures. Part II has no clear interface with GaAs buffer layer, which indicates the good epitaxy conditions. But relaxation occurs at the interface between Part I and Part II. Some CrAs compound (Part I) has

deformed into other phase. In our previous work, we detected the room-temperature ferromagnetism not only in zinc-blende CrAs films but also in the deformed ones,[22] which will help us to understand the inconsistent thickness of sample C. Both the zinc-blende and deformed CrAs compounds exhibit room-temperature ferromagnetism which has been discussed before.[22,23]

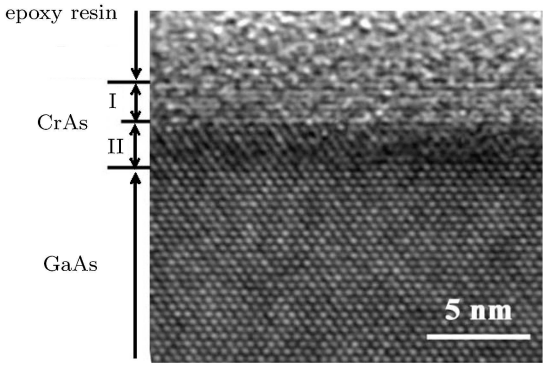


Fig.6. High-resolution cross-sectional transmission electron micrograph images of sample C.

4. Summary

We have systematically investigated the thickness and substrate temperature dependence of the structure, surface morphology and magnetic property of CrAs films. For CrAs films with the thickness of 1, 3 and 5.6 nm, we find that with the increase of the thickness, the structure of CrAs compound film shows the trend relaxed from zinc-blende to another stable phase. The substrate temperature affects the surface morphology and magnetic property obviously. At lower temperature (150 °C), lower saturation magnetization and remanent magnetization are measured. At higher temperature (350 °C), the relaxation occurs. We optimize the substrate temperature to be 250 °C.

Acknowledgments

The authors acknowledge Professor Z.C. Niu, Professor F.H. Yang and Professor H.Z. Zheng for useful discussion.

References

[1] de Groot R A, Mueller F M, van Engen P G and Buschow K H J 1983 *Phys. Rev. Lett.* **50** 2024
[2] Yanase A and Shiratori K 1984 *J. Phys. Soc. Janpan* **53** 312
[3] Schwarz K 1986 *J. Phys. F: Met. Phys.* **16** 211
[4] Pickett W E and Singh D J 1996 *Phys. Rev.* B **53** 1146
[5] Sato K, Katayama and Yoshima H 2002 *Semicond. Sci. Technol.* **17** 367
[6] Braden J G, Parker J S, Xiong P, Chun S H and Samarth N 2003 *Phys. Rev. Lett.* **91** 056602
[7] Shrai M 2004 *J. Phys.: Condens. Mater.* **16** 5525
[8] Chen X S, Guo X G, Lu W, Sun L Z, Sun Y L and Zhou X H 2004 *Acta Phys. Sin.* **53** 1516 (in Chinese)
[9] Chen Y F 2007 *Acta Phys. Sin.* **56** 060941 (in Chinese)
[10] Liu B G 2003 *Phys. Rev.* B **67** 172411
[11] Galanakis I 2002 *Phys. Rev.* B **66** 012406
[12] Shirai M 2003 *J. Appl. Phys.* **93** 6844
[13] Pask J E, Yang L H, Fong C Y, Pickett W E and Dag S 2003 *Phys. Rev.* B **67** 224420
[14] Sanyal B, Bergqvist L and Eriksson O 2003 *Phys. Rev.* B **68** 054417
[15] Akinaga H, Manago T and Shirai M 2000 *Jpn. J. Appl. Phys.* **39** 1118
[16] Ono K, Okabayashi J, Mizuguchi M, Oshima M, Fujimori A and Akinaga H 2002 *J. Appl. Phys.* **91** 8088
[17] Mizuguchi M, Akinaga H, Manago T, Ono K, Oshima M, Shirai M, Yuri M, Lin H J, Hsieh H H and Chen C T 2002 *J. Appl. Phys.* **91** 7917
[18] Zhao J H, Matsukura F, Takamura K, Chiba D, Ohno Y, Ohtani K and Ohno H 2003 *Mater. Sci. Semi. Proc.* **6** 507
[19] Mizuguchi M, Ono K, Oshima M, Okabayashi J, Akinaga H, Manago T and Shirai M 2002 *Surf. Rev. Lett.* **9** 331
[20] Mizuguchi M, Akinaga H, Manago T, Ono K, Oshima M and Shirai M 2002 *J. Magn. Magn. Mater.* **239** 269
[21] Berger P R, Chang K, Bhattacharya P, Singh J and Bajaj K K 1988 *Appl. Phys. Lett.* **53** 684
[22] Bi J F, Zhao J H, Deng J J, Zheng H Z, Li S S, Wu X G and Jia Q J 2006 *Appl. Phys. Lett.* **88** 142509
[23] Etgens V H, de Camargo P C, Eddrief M, Mattana R, George J M and Garreau Y 2004 *Phys. Rev. Lett.* **92** 167205